Engineered Science
DOI: https://dx.doi.org/10.30919/es1395

# Underwater Coaxial Laser-Waterjet Micromachining of Titanium

Wisan Charee,[1] Huan Qi,[2, 3] Hao Zhu[4] and Viboon Saetang[3,5,*]

## Abstract

Thermal damage is a crucial issue in laser micromachining process, so liquid-assisted laser ablation techniques have been developed to overcome this challenge. This study presents the underwater coaxial laser-waterjet micromachining process, which combines the advantages of the waterjet-assisted laser and underwater laser ablation techniques. Titanium was selected as a work sample in this study, where the effects of waterjet flow rate and laser traverse speed on groove width, groove depth, and heat-affected zone (HAZ) were investigated. The influences of the flow rate on the flushing of cut particles and laser beam scattering were also examined to determine the critical flow rate for minimizing the laser beam interference in water. The waterjet flow rate of 250 mL/min was found to be an optimum level, at which a deep groove with a minimum HAZ and clean ablated surface was achievable by the proposed process. Using the flow rate greater than this level in turn caused more laser beam scattering due to the formation of cavitation bubbles and then resulted in the decreased groove dimensions. According to the findings of this study, the proposed coaxial laser-waterjet ablation technique can be another promising process for precisely and damage-free cutting heat-sensitive materials in manufacturing.

*Keywords:* Laser; Waterjet; Underwater; Micromachining; Titanium.
Received: 12 December 2024; Revised: 08 January 2025; Accepted: 21 January 2025.
Article type: Research article.

## 1. Introduction

Titanium and its alloys have increasingly been employed in aerospace, biomedical, and automotive industries due to their exceptional properties, including high strength-to-weight ratio, corrosion resistance, and biocompatibility.[1-3] Lasers have been used for cutting the metals both in macro- and in micro-scales due to their high processing speed, good accuracy,[4] and ability to fabricate complex parts.[5,6] However, thermal damage induced by lasers is detrimental to the part quality in terms of distortion, surface defects, and changes in material and mechanical properties.[7-9] Liquid-assisted laser micromachining processes have been developed to minimize heat accumulation and diminish the thermal damage caused by laser ablation.[10] Although many types of liquids can be applied in the process to enhance heat conduction and wettability, water is usually employed as the liquid to cool down the workpiece being cut by a laser due to its high thermal conductivity, recyclability, and non-toxicity. This can limit the size of the heat-affected zone (HAZ), recast formation, and part distortion. Adding water to the laser ablation process also intensifies the shock pressure caused by the confined plasma plume and the collapse of cavitation bubbles.[11,12] This significantly enhances the material removal rate through the mechanical shock in addition to the typical vaporization mechanism. Moreover, laser ablation in water can reduce smoke and aerosols in the atmosphere, making the technique effective for sensitive environments such as nuclear component cutting.[13]

There are various ways of applying water to the laser ablation process. The whole workpiece can be submerged in water,[14] or only the work surface to be ablated is covered by a layer of water film.[15] The former setup is commonly known

[1] *Department of Industrial Engineering, Faculty of Industry and Technology, Rajamangala University of Technology Isan, Sakon Nakhon, 47160, Thailand*
[2] *College of Engineering, Hangzhou City University, Hangzhou, 310015, China*
[3] *Zhejiang-Thailand International Joint Laboratory on New Materials Digital Design and Processing Technology, Hangzhou City University, Hangzhou, 310015, China*
[4] *School of Mechanical Engineering, Jiangsu University, Zhenjiang, 212013, China*
[5] *Department of Production Engineering, Faculty of Engineering, King Mongkut's University of Technology Thonburi, Bangkok, 10140, Thailand*
[*] *Email:* viboon.tan@kmutt.ac.th (V. Saetang)

as the underwater laser ablation. This method provides the cooling effect, which mitigates the HAZ, reduces thermal damage, and minimizes residual stresses in the laser-ablated parts.[16,17] The incorporation of ultrashort-pulse lasers, such as femtosecond-pulse lasers, into liquid-assisted laser ablation has further expanded the process capabilities. These lasers emit very short pulse duration and keep energy deposition to an extremely short period of time, thus minimizing heat transfer towards the work material and reducing thermal damage accordingly.[18] Another promising area in liquid-assisted laser ablation is the use of ionic liquids. Due to their low vapor pressures and high thermal stability, ionic liquids are highly effective at controlling laser-induced cavitation and minimizing thermal damage. Canfield *et al*.[19] explored the use of ionic liquids in an ultrafast laser micromachining process, finding that the liquid provides greater control over material removal processes, especially for brittle materials. Using ionic liquids to assist the laser micromachining process could offer new possibilities for high-precision and damage-free microfabrication.

The effect of water flow rate in the underwater laser micromachining process is a critical factor affecting machining quality and material removal rate. Compared with the laser ablation in still water, the applying of water flow across the workpiece surface helps the flushing of cut debris and improves the workpiece cooling.[10] Wang *et al*.[20] found that the optimal water flow rate of 8 m/s leads to better surface quality and effective debris removal as the water flow minimizes excessive heat buildup and prevents damage to the workpiece. Lin *et al*.[21] corroborated this by showing that underwater drilling with an ultrashort-pulse laser is more efficient than in-air drilling, owing to the cooling effect of water flow. Dowding and Lawrence emphasized that higher water flow rates facilitate efficient debris flushing, which prevents laser beam interference and ensures better ablation accuracy.[22] Moreover, the study by Yuhong *et al*.[23] showed that in brittle material removal, the water flow enhances the impact of shock forces, thus increasing the material removal rate. Long *et al*.[24] extended these findings by demonstrating how water flow combined with nonuniform surface wettability improves the underwater laser micro-grooving process, and they found that using fast water flow can provide good machining accuracy.

In addition to the underwater approach, water can be supplied to the laser ablation process as a jet, such as the waterjet-guided laser and hybrid laser-waterjet technology.[25,26] These processing techniques have proven effective in achieving negligible HAZ and better-cut surface quality than laser ablation in ambient air or even in still water.[27-31] A waterjet is used in conjunction with a laser beam to cool the material and remove ablated debris. As for the waterjet-guided laser technology, the waterjet and laser beams are coaxially aligned to become a single beam due to the total internal reflection of the laser in water. However, the processing performance of this technology is greatly dependent on the waterjet beam. The jet diameter has to be as small as possible to intensify the fluence of the laser, reflecting in the waterjet beam for maximizing the ablation rate. Moreover, the laser used for this technology has to have its wavelength fitted for transmitting in water with minimum loss. Therefore, the process has to be operated at a very high water pressure to create a fine diameter of the continuous laser-waterjet beam, and no lasers are applicable for this ablation technique.

This paper presents a more robust laser-waterjet micromachining process than the existing water-assisted laser ablation techniques. The process combines the advantages of the waterjet-assisted laser ablation and underwater approach to enhance the flushing of cut particles and bubbles by a localized waterjet and to cool the entire workpiece by submerging it in water. The proposed technique uses a coaxial alignment of the laser beam and waterjet, directing both simultaneously onto the workpiece surface in water. Unlike the waterjet-guided laser, a larger waterjet nozzle is used in this study to enable the operation of a lower-pressure pump. In addition, the laser beam is not required to be subjected to the total internal reflection with a long traveling distance in the waterjet beam but directly focuses on the workpiece submerged in water. Thereby, the ablation is mostly dependent on the laser beam in terms of the control of laser fluence and beam diameter, whereas the waterjet is responsible for cooling down the workpiece, preventing the deposition of cut debris on the work surface, and promoting the material removal rate. The effects of waterjet flow rate and laser traverse speed on cut dimensions and quality are to be investigated in this study. The synergy between the laser and waterjet in the proposed ablation technique is expected to enhance the material removal efficiency and minimize thermal damage, leading to superior surface quality and dimensional accuracy. This study not only contributes to the advancement of laser micromachining technology but also provides valuable insights into the potential applications and benefits of integrating laser and waterjet in high-precision and damage-free manufacturing.

## 2. Materials and methods

A pure titanium sheet having a thickness of 1 mm was grooved by a nanosecond-pulse laser (YLP-1-100-30-30-HC-RG, Germany) in this study. The workpiece was clamped by a stainless-steel fixture and submerged in water. A coaxial laser-waterjet cutting head was positioned above the workpiece surface, as shown in Fig. 1(a). The top side of the cutting head chamber was a 2-mm thick fused silica window through which a laser beam transmits from a laser source. The laser wavelength, pulse repetition rate, and pulse duration were 1064 nm, 30 kHz, and 100 ns, respectively. The laser beam coaxially passed through a 1-mm diameter waterjet nozzle placed on the bottom side of the chamber. The waterjet flow rate was subject to the inlet flow induced by a diaphragm pump. The gap distance between the nozzle exits and the workpiece surface or nozzle stand-off distance was kept

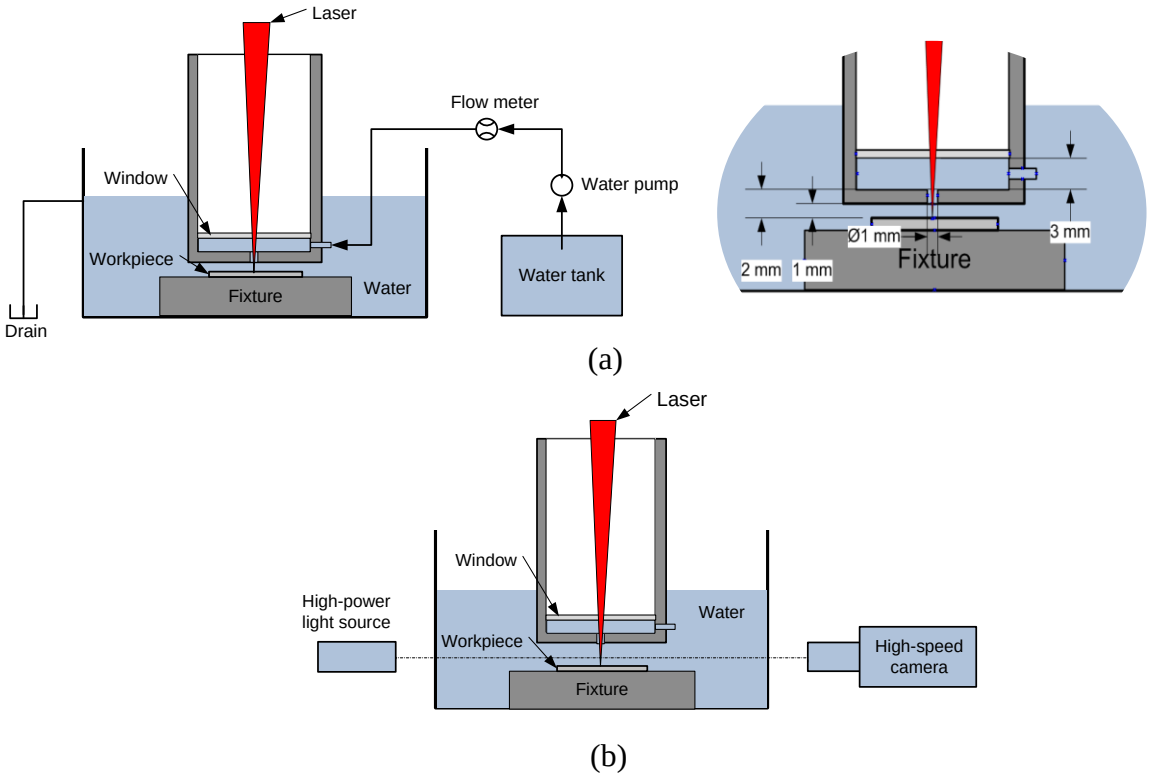


**Fig. 1:** Experimental setup of (a) the coaxial laser-waterjet cutting head and (b) the high-speed camera.

constant at 1 mm, and the total length of the laser path in water starting from the bottom side of the fused silica window to the workpiece surface was 5 mm. With this setup, the workpiece can be ablated by the coaxial laser-waterjet beam in water.

The laser beam distribution was Gaussian, and the beam was subjected to optical refraction at the air-window and window-water interfaces due to the laser-waterjet coupling. The diameter of the laser beam ($d_b$) irradiating on the workpiece surface can be calculated by using Eq. (1):

$$d_b = \frac{2\lambda M^2}{\pi \tan\theta_w}\left\{1+\left[\frac{(h_g+h_w)D/2F - h_g\tan\theta_g - h_w\tan\theta_w}{z_R\tan\theta_w}\right]^2\right\}^{1/2} \quad (1)$$

where $\lambda$, $M^2$, $h_g$, $h_w$, $D$, and $F$ are the laser wavelength, laser beam quality (1.5), thickness of fused silica window (2 mm), distance of laser beam traveling in water (5 mm), collimated laser beam diameter at the entrance of focusing lens (7.5 mm), and the focal length of focusing lens (254 mm). $z_R$ is the Rayleigh length, which is calculated by using Eq. (2):

$$z_R = \frac{\lambda M^2}{\pi \tan^2\theta_w} \quad (2)$$

where $\theta_g$ and $\theta_w$ are the angles of the refracted laser in the fused silica window and in water. These can be determined by Eqs. (3)-(4):

$$\theta_g = \sin^{-1}\left\{\frac{\sin[\tan^{-1}(D/2F)]n_a}{n_g}\right\} \quad (3)$$

$$\theta_w = \sin^{-1}\left[\sin\left(\sin^{-1}\left\{\sin\left[\tan^{-1}\left(\frac{D}{2F}\right)\right]\frac{n_a}{n_g}\right\}\right)\frac{n_g}{n_w}\right] \quad (4)$$

where $n_a$, $n_g$, and $n_w$ are the refractive index of air (1.0), fused silica window (1.450), and water (1.325), respectively. According to Eq. (1), the calculated diameter is 106.26 µm.

Since this technique combines a laser beam with a jet of water, the process parameters and their effect on the ablation performance regarding the laser-waterjet coupling and microgrooving process have to be investigated. The average laser power employed in this study was set at 30 W, which was the maximum power of the laser machine. Two key parameters taken into account in this study were laser traverse speed and water flow rate. A motorized linear stage was used for translating the whole water container with the submerged workpiece at a given traverse speed. The speed was varied from 20 to 60 mm/min with a step size of 20 mm/min. Fifteen levels of water flow rate starting from 25 to 550 mL/min were applied in the experiment, as listed in Table 1. With 45 experimental conditions and five repetitions for each, a total of 225 experiments were conducted to ensure consistency and statistical validity. These values were chosen based on the applicable limit of the water pump. Regarding the nozzle diameter of 1 mm, the waterjet velocity at the nozzle exit was varied from 0.53 to 11.67 m/s. The width, depth, and heat-affected zone of each groove obtained from the experiment were observed and quantified by a digital microscope (Nikon SMZ25, Japan). In addition, a high-speed camera (Fastcam mini ux100 type 200k-m-16g) operating at 10,000 frames per second, as illustrated in Fig. 1(b), was employed to in situ observe the dynamic behaviors of laser-induced bubbles and flushing of cut debris in the underwater coaxial laser-waterjet ablation process.

## 3. Results and discussion

### 3.1 Comparison between the laser ablation in air, in water, and in water with the coaxial laser-waterjet technique

Before fully investigating the underwater coaxial laser-waterjet micromachining process, the titanium sheet was grooved by the laser in air and in water with and without using the coaxial laser-waterjet technique for comparison purposes. This comparative analysis aimed to discern the specific effects of air and water as well as the coaxial laser-waterjet roles on the quality of laser-grooved channels. The laser power and laser traverse speed were set to 30 W and 1 mm/s, respectively, across all experiments. The workpiece was submerged at a depth of 5 mm for the underwater conditions. The water flow rate of 25 mL/min was applied in the case of the coaxial laser-waterjet method.

**Table 1:** Parameters considered in the experiment.

| Process parameters | Values |
|---|---|
| Water flow rate (mL/min) | 25, 50, 75, 100, 125, 150, 175, 200, 250 300, 350, 400, 450, 500, and 550 |
| Laser traverse speed (mm/min) | 20, 40, and 60 |
| Average laser power (W) | 30 |

The morphology of grooves resulting from the laser ablation in the three different conditions is presented in Fig. 2. No distinct groove formation was found when performing the ablation in air and in water without the aid of the coaxial laser-waterjet. High recast structures and oxides were evident on the workpiece surface (Fig. 2(a)), where the dry laser ablation was applied. On the other hand, the recast was minimized when the ablation was done in water, as shown in Fig. 2(b). Two mechanisms are responsible for this improvement. Firstly, the surrounding water helps the workpiece cool down faster than in the air. This can limit the amount of heat to accumulate and enlarge the laser-molten region where the recast is later formed after solidification. The optical absorption in water is another mechanism causing small recast formation. The laser beam traveling in water undergoes intensity loss according to Beer-Lambert's law.[32] At the laser wavelength of 1064 nm, the absorption coefficient of water was approximately 0.135 $cm^{-1}$.[33,34] With a water depth of 5 mm, the intensity loss is about 6.5%. This still does not include losses caused by the reflection at the air-water interface, disturbance of bubbles and plasma plume generated during the laser ablation in water, and interference of water droplets splashing from the ablation area. The significant loss of laser intensity not only reduces the recast structure but also diminishes the material removal.

When the coaxial laser-waterjet technique was applied in the underwater laser ablation, a remarkable groove was formed with negligible recast structures, as shown in Fig. 2(c). Although the travel length of the laser beam in water was the same 5 mm as that used in the underwater setup, the laser intensity losses induced by the other factors except for the direct absorption of 6.5% were totally omitted. The laser beam scattering and reflection due to water waves and atomized water droplets at and above the air-water interface are neglected. This is because the coaxial laser-waterjet cutting head was equipped with a protective window, so the flat interface and free of water splashing disturbance can be attained accordingly. Although the fused silica window

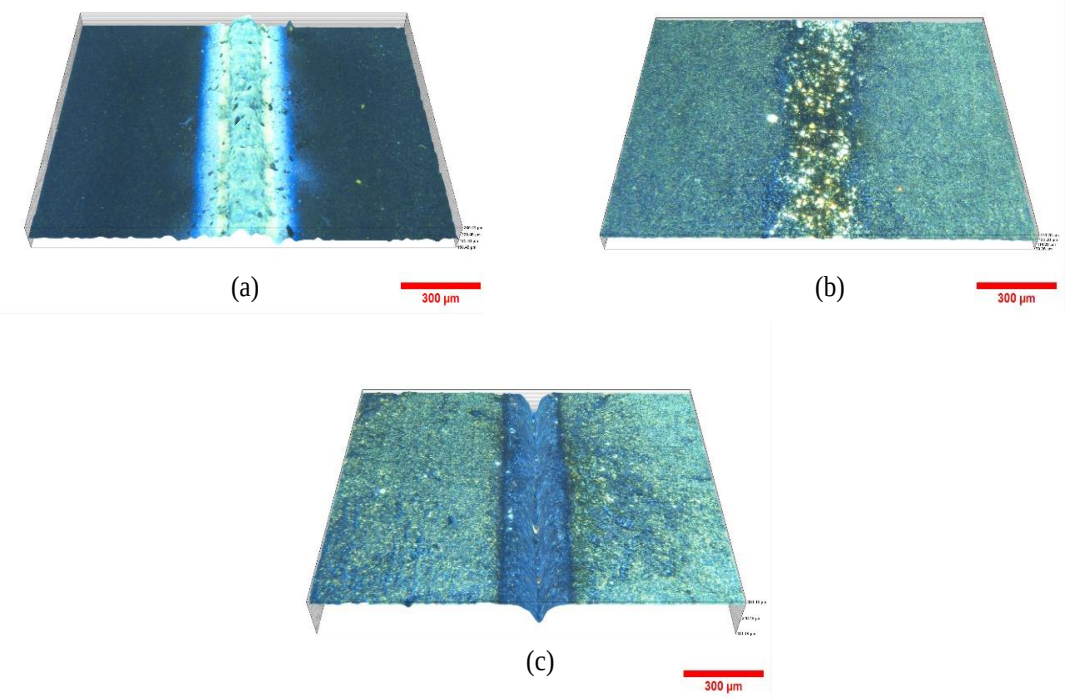


**Fig. 2:** Surface morphology of grooves caused by the laser ablation: (a) in air, (b) in water, and (c) in water with the coaxial laser-waterjet technique (water flow rate = 25 mL/min).

introduces loss to the laser beam passing through it, the loss is less than 3% at the applied laser wavelength.[35] This is indeed much lower than the losses caused by the dynamic air-water interface and water splashing. The laser intensity as well as the beam quality reaching the workpiece surface in water can be greater than that of the typical underwater laser ablation, and so more material can be removed. Another contribution of the coaxial laser-waterjet technique comes from the water flow at the nozzle exit. This helps the flushing of cut debris, pushing gas bubbles and plasma away from the ablation zone, and better cooling the workpiece than still water. In addition, the jet of water introduces an impact force to substantially promote the removal of the molten layer from the groove bottom. This thereby enables a deeper groove formation by allowing the laser beam to further ablate the workpiece without being impeded by the molten layer. Therefore, the underwater coaxial laser-waterjet micromachining technique developed in this study is viable and has a high potential for enhancing the material removal rate and bettering the cut quality compared to the typical laser ablation methods.

### 3.2 Effects of water flow rate and laser traverse speed

The surface morphology and profile of grooves produced by the coaxial laser-waterjet ablation in water are shown in Fig. 3. It is apparent from Fig. 3 that no substantial protrusion of recast structures is formed along the groove's edges as for the applied range of water flow rate. In addition to the clean groove surface, the groove width and depth were found to change with the water flow rate. Figs. 4(a) and 4(b) present the relationship between the water flow rate, laser traverse speed, and groove sizes. An increase in the laser traverse speed reduced the groove width and depth. This is due to the laser energy density that decreases with the increased speed. The low energy density results in less melting and removal of work material. This relationship is typical and can be found in many studies on laser material processing.[36] Since the Gaussian laser beam was used in this study, the laser energy density is maximum at the center of the beam profile and radially decreases away from the beam center. The thermal conduction in the material also distributes as an exponential function in the spatial domain.[37] The thermal energy near the groove center, whose level is greater than the ablation threshold of the material, results in the groove formation through the vaporization mechanism. By contrast, the thermal energy of less than the ablation threshold causes partial melting or insignificant material removal to the work surface. This region was defined as the HAZ in this study. The HAZ width is found to be large when the high laser traverse speed is applied together with the low water flow rate, as shown in Fig. 4(c). The use of high traverse speed limited the groove formation close to the beam center, so the large area of partial melting/ablation around the groove channel was treated as the HAZ. When the traverse speed became slower, the groove boundary expanded, and the HAZ tended to be smaller compared to the groove width. The heat accumulation induced by the slow traverse speed caused some parts of HAZ to vaporize where their energy was higher than the ablation threshold. However, when the applied water flow rate was greater than 250 mL/min, the effect of the traverse speed on the HAZ width was insignificant. The overall HAZ, as well as the groove dimensions, was found to reduce with the increased water flow rate, at which the thermal convection became a dominant factor in the process.

The effects of the water flow rate on the groove width and depth are shown in Figs. 4(a) and 4(b) are interesting. The groove sizes increased with the flow rate and then decreased after a flow rate of 250 mL/min. This changing trend is subject to two major roles of water flow in assisting the laser ablation in water, and a trade-off between them causes a turning point in the results. Firstly, the water flow provides an effective flushing of cut debris and bubbles generated in water to not block the laser beam during the ablation. This importantly reduces the laser intensity loss and scattering due to the blockage and maintains the beam quality throughout the ablation in water. Secondly, a higher water flow offers a better cooling action to the workpiece through the convection mechanism. This helps the HAZ reduction and excessive heat accumulation in the laser-ablated region. However, the use of a too high flow rate can decrease the material removal rate as well as the groove dimensions to some extent.

Regarding the flushing issue, the cut particles, including the gas bubbles, have to be pushed out by the water flow from the laser ablation zone during the laser pulse-off time period. To cope with this condition, the water flow velocity has to be greater than a critical velocity ($v_w^*$; m/s), which is determined by Eq. (5):

$$v_w^* = f \cdot d_b \tag{5}$$

where $f$ and $d_b$ are the laser pulse repetition rate (30 kHz) and laser beam diameter (106.26 μm). According to Eq. (5), the critical water flow velocity was 3.188 m/s. The critical water flow rate ($V_w^*$; mL/min) is thus calculated by using Eq. (6):

$$V_w^* = 15\pi v_w^* d_{wj}^2 10^6 \tag{6}$$

where $d_{wj}$ is the diameter of the waterjet nozzle (1 mm). With regard to the flow velocity of 3.188 m/s, the critical water flow rate is 150.222 mL/min. Hence, any particles suspended in the laser-projected area can be flushed away without impeding the subsequent laser pulse when using this critical flow rate. Although this is an underestimated situation in which the particles are assumed to be moved at the same speed and same direction of water flow, it can be used as a guideline for choosing an effective water flow rate in assisting the laser ablation in water.

Regarding the groove width and depth shown in Figs. 4(a) and 4(b), the sizes increase with the flow rate and slightly change after reaching the critical level. This indicates the contribution of the water flow in flushing the particles away from the ablation zone. As per the results, the maximum groove dimensions were obtained at a water flow rate of about 200-250 mL/min. This is slightly higher than the critical flow rate of 150.222 mL/min. As aforementioned, the critical flow

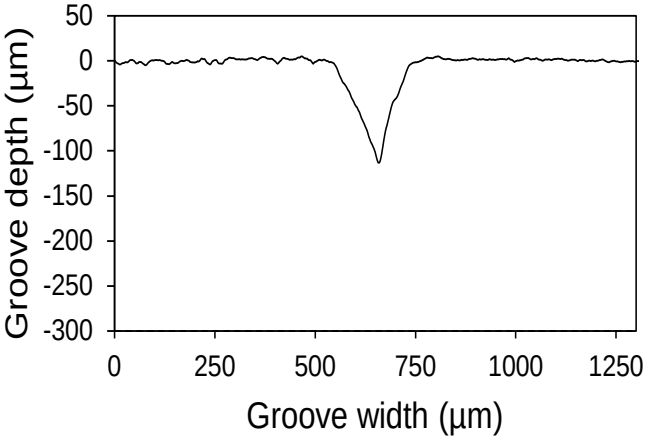


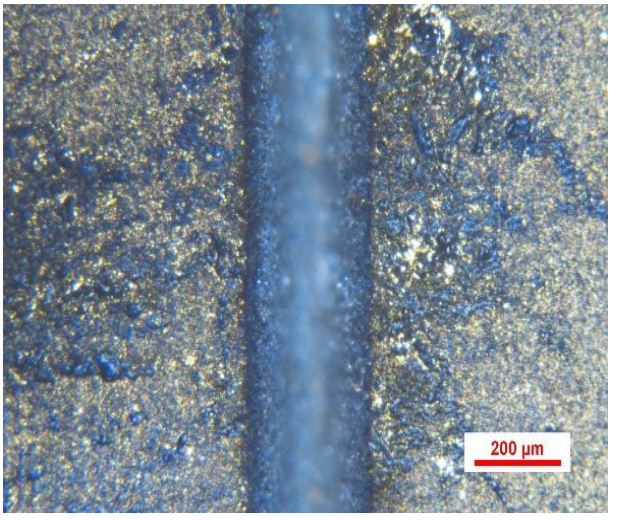


(a)

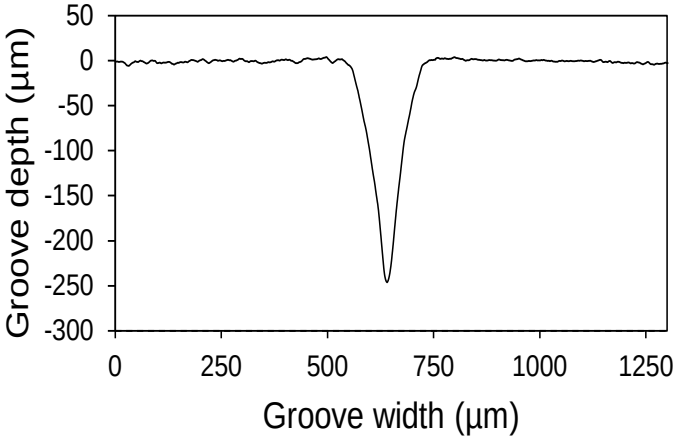


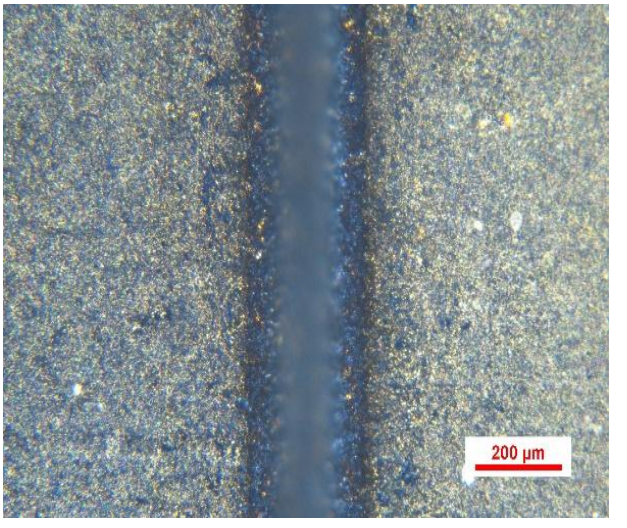


(b)

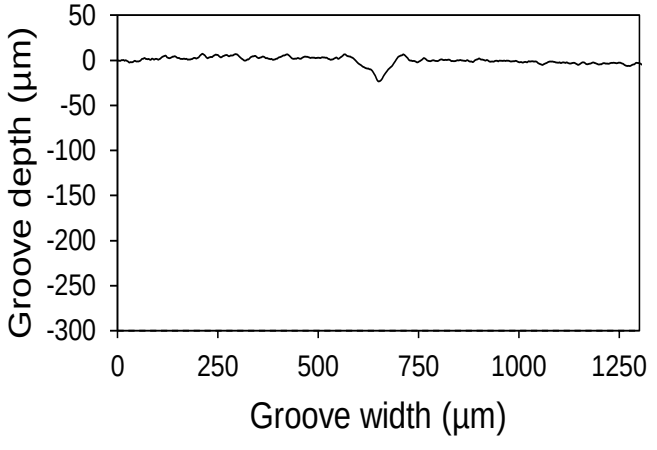


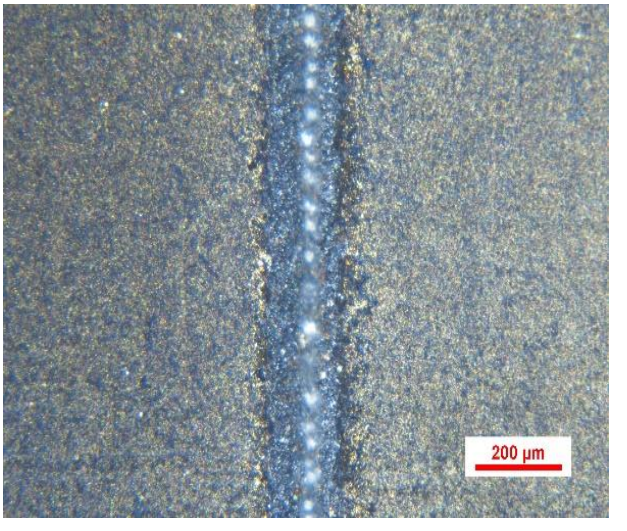


(c)

**Fig. 3:** Groove produced by the underwater coaxial laser-waterjet micromachining process when using the laser traverse speed of 20 mm/min and water flow rate of: (a) 25 mL/min, (b) 250 mL/min, and (c) 550 mL/min.

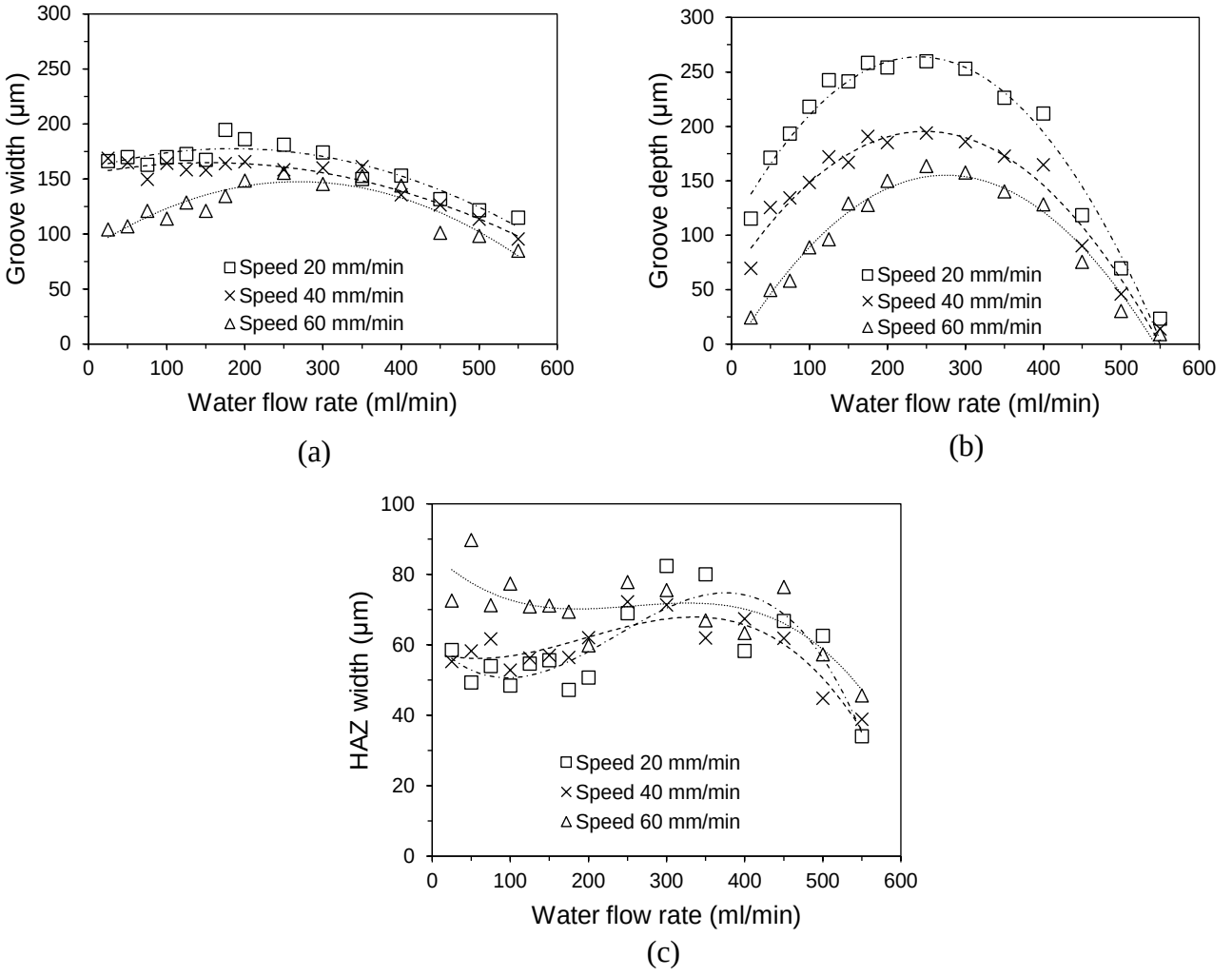


**Fig. 4:** (a) Groove width, (b) depth , and (c) HAZof titanium obtained under the different processing conditions.

rate expressed in Eq. (6) is underestimated and it relies on the assumption that the particle speed is the same as the water flow. However, there are some situations in which a higher flow rate than the critical value is required. Firstly, the cut debris and bubbles ejected from the ablation zone due to shock pressure and vaporization have their own speed and direction.[12,38] Some particles whose ejecting direction is not parallel to the water flow direction can still exist in the laser-projected area and then impede the subsequent laser pulse. Secondly, some gas bubbles can adhere to the workpiece surface near the ablation zone due to a strong adhesion force. When the laser beam moves to the area with bubble adhesion, optical interference takes place and limits the ablation performance. A higher water flow rate than the critical value may be needed to push the bubbles further away from the ablation zone and vicinity in order to not land and adhere to the workpiece surface being ablated by the subsequent laser pulses. Lastly, the dislodgement of laser-molten material in the middle of the laser pulse-off time is another uncontrollable factor interfering with the next laser pulse. At a certain flow rate, a significant shear force induced by the flow can expel the laser-molten material from the workpiece. This can even happen during the laser pulse-off time period, in which the dislodged elements are unable to flow away from the ablation zone before the next laser pulse starts. This thereby results in the optical disturbance in the subsequent ablation.

A high-speed camera was employed to observe the flushing of cut particles during the coaxial laser-waterjet ablation in water, and some captured images are depicted in Fig. 5. To realize the flushing behavior, a particular bubble, which was able to be identified more easily than tiny cut debris, was tracked at each time step of 0.1 ms as per the high-speed camera images, and its positions were recorded. The bubble positions subjected to the three water flow rates are shown in Fig. 6(a). It can be noted from Figs. 5 and 6(a) that the bubbles are more pushed away from the ablation zone by a higher water flow. When using the flow rate of 250 mL/min which is greater than the critical flushing rate of 150.222 mL/min, the laser beam scattering was found to reduce compared to the use of the 25-mL/min flow rate. This observation hence supports our discussion on the flushing effect and the critical water flow rate. Regarding Fig. 6(a), the bubble flow velocity was calculated, and its average velocity is plotted in Fig. 6(b). It is interesting to note that the bubble flow velocity is substantially lower than the water flow velocity, as shown in Fig. 6(b). This corresponds with our aforementioned assumption that the

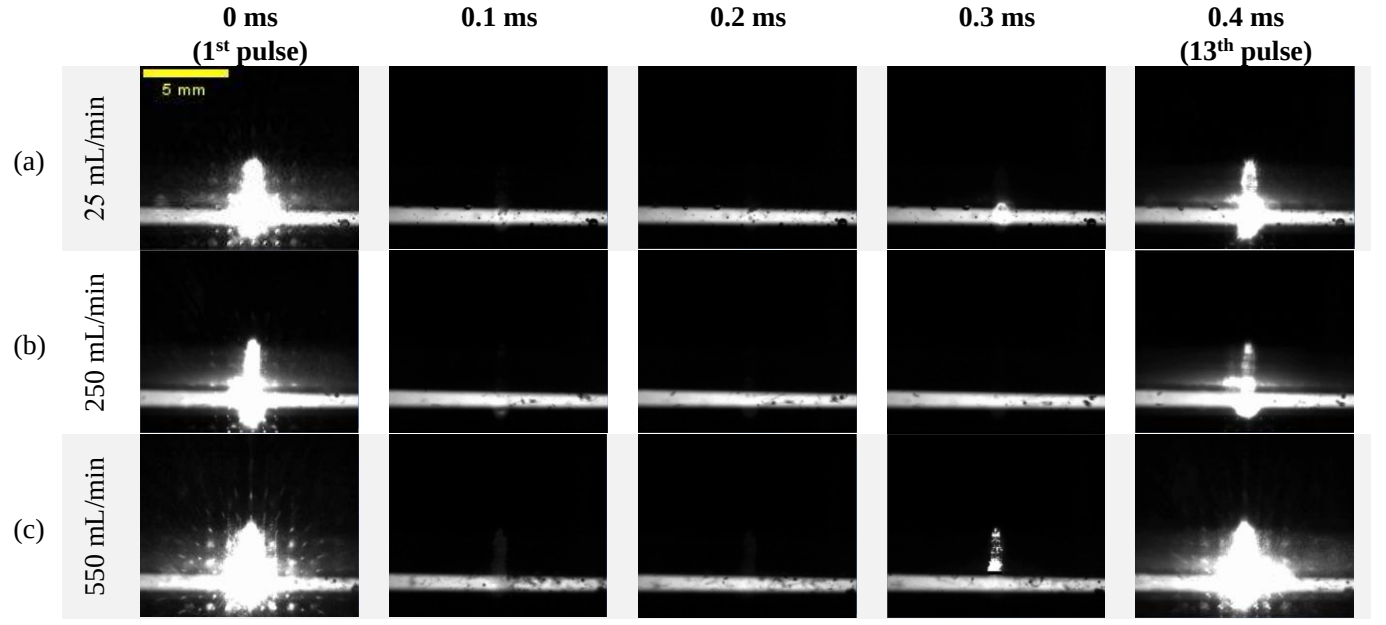


**Fig. 5:** Water flushing of particles during the coaxial laser-waterjet ablation in water when using the flow rates of (a) 25, (b) 250, and (c) 550 mL/min.

bubbles have their initial speed and direction due to the magnitude and direction of shock pressure as well as the vaporization, so the critical flow velocity of 3.188 m/s is an underestimated value. At this velocity, small particles can mostly be flushed away from the ablation zone, but some large particles, such as bubbles, may still interfere with the subsequent laser pulses. Therefore, a higher flow velocity is required to flush all particles from the ablation zone before irradiating the next laser pulse. Although the use of a 550-mL/min flow rate can push bubbles farther from the ablation zone, as shown in Fig. 6(b), the laser beam scattering presented in Fig. 5 is adversely more than at the flow rate of 25 mL/min. More particles were found in water, and they were believably responsible for the significant laser beam scattering. The particles found above the workpiece surface when using the flow rate of 550 mL/min were mostly cavitation bubbles. Using this flow rate, the local pressure in the 1-mm gap between the workpiece surface and nozzle tip potentially decreases below the saturated vapor pressure of water, thus generating more cavitation bubbles. Therefore, the reduction of groove dimensions at the high flow rate was subject to not only the high thermal convection but also the laser beam scattering induced by the cavitation bubbles. According to Fig. 4, the processing window of the recommended water flow rate to maximize the groove dimensions approximately ranges from 150 to 350 mL/min, and the flow rate providing the largest groove is 250 mL/min. These findings can be an essential guideline for choosing the suitable water flow rate in the coaxial laser-waterjet ablation technique and are plausibly applicable to other liquid-assisted laser ablation processes.

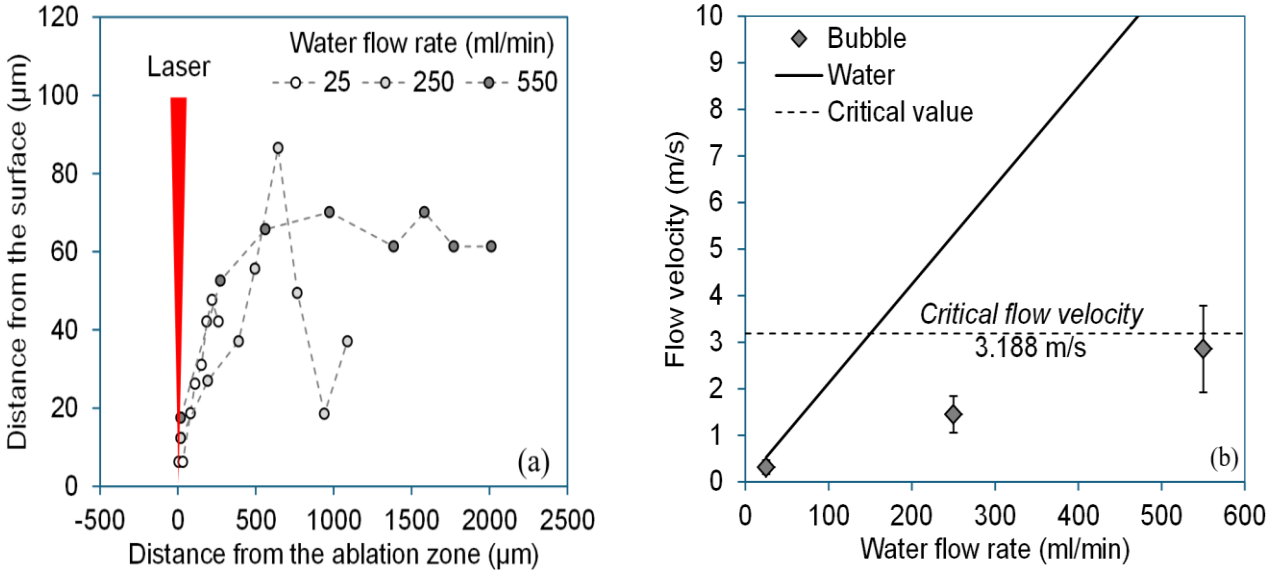


**Fig. 6:** Effect of water flow rate: (a) bubble tracking every 0.1-ms time step and (b) bubble and water flow velocities.

## 4. Conclusion

This study proposed the underwater coaxial laser-waterjet micromachining process for grooving titanium. The effects of waterjet flow rate and laser traverse speed on the groove dimensions and HAZ were investigated. The key findings can be drawn as follows:

1. The coaxial laser-waterjet ablation technique significantly enhanced both debris removal and cooling compared to laser micromachining in air or still water. The waterjet effectively removed cut particles and bubbles from the cutting zone, thus promoting continuous and efficient material removal. The synergy between the laser and waterjet also reduced the formation of recast structures on the workpiece surface, leading to high-quality surface finishes with minimal defects.
2. The waterjet flow rate had a significant impact on the groove dimensions and also played a crucial role in minimizing the HAZ. The optimum flow rate of approximately 250 mL/min was able to maximize both the groove width and depth due to the effective flushing of cut debris and bubbles from the cutting zone. Although using the water flow rate of greater than 250 mL/min further reduced the HAZ along the cut, a significant decrease in groove dimensions was observed. This reduction was attributed to the excessive cooling and the scattering of the laser beam by cavitation bubbles, thus reducing the material removal.
3. The use of higher laser traverse speeds increased the likelihood of larger HAZ formation, particularly at lower water flow rates, due to heat accumulation and insufficient cooling. This suggests a trade-off between traverse speed and thermal damage control.
4. The findings of this study highlighted the importance of balancing the waterjet flow rate to maximize material removal and minimize thermal damage during the underwater laser-waterjet ablation. These provide valuable insights into achieving high-quality micromachining with minimal HAZ for medical and aerospace industries where precision and minimal thermal impact are the critical concerns.

## Acknowledgment

This research was supported by Science Research and Innovation Fund. Contract No. FF66-P1-038; National Natural Science Foundation of China (52275431); King Mongkut's University of Technology Thonburi (KMUTT), Thailand Science Research and Innovation (TSRI), and National Science, Research and Innovation Fund (NSRF) Fiscal year 2025 Grant number (FRB680074/0164).

## Conflict of Interest

There is no conflict of interest.

## Supporting Information

Not applicable.

## References

[1] C. N. Elias, J. H. C. Lima, R. Valiev, M. A. Meyers, Biomedical applications of titanium and its alloys, *JOM*, 2008, **60**, 46-49, doi: 10.1007/s11837-008-0031-1.
[2] A. K. Sachdev, K. Kulkarni, Z. Z. Fang, R. Yang, V. Girshov, Titanium for automotive applications: challenges and opportunities in materials and processing, *JOM*, 2012, **64**, 553-565, doi: 10.1007/s11837-012-0310-8.
[3] J. C. Williams, R. R. Boyer, Opportunities and issues in the application of titanium alloys for aerospace components, *Metals*, 2020, **10**, 705, doi: 10.3390/met10060705.
[4] D. Raj, B. V. R. Reddy, S. R. Maity, K. M. Pandey, Laser beam micromachining of metals: a review, *Materials Today: Proceedings*, 2019, **18**, 98-103, doi: 10.1016/j.matpr.2019.06.281.
[5] K. Shihoyama, A. Furukawa, P. Bado, Ali A. Said, Micromachining with ultrafast lasers, *Proceedings SPIE*, 2000, **4088**, 1-4, doi: 10.1117/12.405701.
[6] A. Nebel, T. Herrmann, B. Henrich, R. Knappe, Fast micromachining using picosecond lasers, *Proceedings SPIE*, 2005, **5706**, 87-98, doi: 10.1117/12.601651.
[7] K. Garasz, M. Kocik, R. Barbucha, M. Tanski, J. Mizeraczyk, M. Nejbauer, C. Radzewicz, A prototype femtosecond laser system for precise micromachining, 2012 Symposium on Photonics and Optoelectronics, May 21-23, 2012, Shanghai, China, IEEE, 1-3, doi: 10.1109/SOPO.2012.6271128.
[8] R. S. Patel, J. M. Bovatsek, High speed micromachining with high power UV laser, *Proceedings SPIE*, 2013, **8608**, 1-7, doi: 10.1117/12.2008698.
[9] W. W. Zhang, J. K. Jiao, L. Ruan, T. R. Zhang, Experimental study on laser high-speed micro-processing, *ASME 2014* International Manufacturing Science and Engineering Conference Collocated with the JSME 2014 International Conference on Materials and Processing and the 42nd North American Manufacturing Research Conference, June 9-13, 2014, Detroit, Michigan, USA, doi: 10.1115/MSEC2014-4065.
[10] A. Kruusing, Underwater and water-assisted laser processing: part 1: general features, steam cleaning and shock processing, *Optics and Lasers in Engineering*, 2004, **41**, 307-327, doi: 10.1016/S0143-8166(02)00142-2.
[11] M. Li, H. C. Zhang, Z. H. Shen, J. Lu, X. W. Ni, Physical analyses of optical breakdown and plasma formation in water induced by laser, *Acta Photonica Sinica*, 2005, **34**, 1610-1614.
[12] Y. Guo, P. Qiu, S. Xu, G. J. Cheng, Laser-induced microjet-assisted ablation for high-quality microfabrication, *International Journal of Extreme Manufacturing*, 2022, **4**, 035101, doi: 10.1088/2631-7990/ac6632.
[13] S. Mullick, Y. K. Madhukar, S. Roy, S. Kumar, D. K. Shukla, A. K. Nath, Development and parametric study of a water-jet assisted underwater laser cutting process, *International Journal of Machine Tools and Manufacture*, 2013, **68**, 48-55, doi: 10.1016/j.ijmachtools.2013.01.005.
[14] N. Krstulović, S. Shannon, R. Stefanuik, C. Fanara, Underwater-laser drilling of aluminum, *The International Journal of Advanced Manufacturing Technology*, 2013, **69**, 1765-1773, doi: 10.1007/s00170-013-5141-4.

[15] V. Tangwarodomnukun, P. Likhitangsuwat, O. Tevinpibanphan, C. Dumkum, Laser ablation of titanium alloy under a thin and flowing water layer, *International Journal of Machine Tools and Manufacture*, 2015, **89**, 14-28, doi: 10.1016/j.ijmachtools.2014.10.013.
[16] W. Charee, V. Tangwarodomnukun, Underwater laser turning of commercially-pure titanium, *Key Engineering Materials*, 2020, **861**, 23-27, doi: 10.4028/www.scientific.net/kem.861.23.
[17] J. Y. Lee, D. H. Kim, Y. T. Cho, C. M. Lee, A study on the characteristics of 304 stainless steel according to the water temperature changes in underwater laser beam machining, *Materials*, 2023, **16**, 7463, doi: 10.3390/ma16237463.
[18] H. Yuan, Z. Chen, P. Wu, Z. Zhu, X. Wang, X. Cao, W. Zhang, Research on different medium-assisted quartz material processing technology based on femtosecond laser, *Proceedings SPIE*, 2022, **12507**, 1-5, doi: 10.1117/12.2656050.
[19] B. K. Canfield, J. N. Allman, A. Terekhov, T. M. Moeller, L. Costa, Ionic Liquid-assisted Cavitation for Ultrafast Laser Micromachining, CLEO 2023, San Jose, CA, Optica Publishing Group, 2023, doi: 10.1364/cleo_si.2023.sth1n.3.
[20] X. Wang, Y. Huang, X. Wang, B. Xu, J. Feng, B. Shen, Experimental investigation and optimization of laser induced plasma micromachining using flowing water, *Optics & Laser Technology*, 2020, **126**, 106067, doi: 10.1016/j.optlastec.2020.106067.
[21] J. Lin, K. Yang, R. Xu, M. Xia, T. Huang, Experimental investigation of efficiency of drilling with ultrashort-pulse laser in water, *Proceedings SPIE*, 2002, **4915**, 1-6, doi: 10.1117/12.482864.
[22] C. F. Dowding, J. Lawrence, Ablation debris control by means of closed thick film filtered water immersion, *Proceedings of the Institution of Mechanical Engineers, Part B: Journal of Engineering Manufacture*, 2010, **224**, 753-768, doi: 10.1243/09544054jem1711.
[23] Y. Long, L. Xiong, T. Shi, The research on mechanical effect etching Si in pulsed laser micromaching under water, *Applied Surface Science*, 2011, **257**, 3677-3681, doi: 10.1016/j.apsusc.2010.11.105.
[24] J. Long, Q. Weng, W. Hong, Z. Cao, P. Zhou, X. Xie, Fast water flow in laser micromachined microgrooves with nonuniform surface wettability, *Experimental Thermal and Fluid Science*, 2019, **103**, 9-17, doi: 10.1016/j.expthermflusci.2018.12.031.
[25] B. Richerzhagen, M. Kutsuna, H. Okada, T. Ikeda, Waterjet-guided laser processing, *Proceedings SPIE*, 2003, **4830**, 1-4, doi: 10.1117/12.486514.
[26] V. Tangwarodomnukun, J. Wang, C. Z. Huang, H. T. Zhu, An investigation of hybrid laser–waterjet ablation of silicon substrates, *International Journal of Machine Tools and Manufacture*, 2012, **56**, 39-49, doi: 10.1016/j.ijmachtools.2012.01.002.
[27] T. Nilsson, F. Wagner, R. Housh, B. Richerzhagen, Scribing of GaN wafer for white LED by water-jet-guided laser, *Proceedings SPIE*, 2004, **5366**, 1-7, doi: 10.1117/12.529012.
[28] L. J. Yang, M. L. Wang, Y. Wang, J. Tang, Y. B. Chen, Numerical and experimental research on water-jet guided laser micromachining, *Materials Science Forum*, 2009, **626**, 297-302, doi: 10.4028/www.scientific.net/msf.626-627.297.
[29] C. Q. Li, L. J. Yang, Y. Wang, A research on surface morphology of cutting of titanium sheet with water-jet guided laser and conventional laser, *Applied Mechanics and Materials*, 2011, **120**, 366-370, doi: 10.4028/www.scientific.net/amm.120.366.
[30] H. Zhu, J. Wang, W. Y. Li, H. Z. Li, Microgrooving of germanium wafers using laser and hybrid laser-waterjet technologies, *Advanced Materials Research*, 2014, **1017**, 193-198, doi: 10.4028/www.scientific.net/amr.1017.193.
[31] L. Subasi, J. Diboine, A. Gunaydin, C. Tuzemen, O. C. Ozaner, R. Martin, Water jet guided laser microdrilling of aerospace alloys: Correlation of material properties to process time and quality, *Journal of Laser Applications*, 2021, **33**, 012015, doi: 10.2351/7.0000302.
[32] Z. Wei, Z. Song, R. Song, X. Zhang, Z. Meng, Measurement of the optical absorption coefficient for liquid based on optical microfiber, *Optik*, 2014, **125**, 2880-2884, doi: 10.1016/j.ijleo.2013.11.048.
[33] S. Mullick, Y. K. Madhukar, S. Kumar, D. K. Shukla, A. K. Nath, Temperature and intensity dependence of Yb-fiber laser light absorption in water, *Applied Optics*, 2011, **50**, 6319, doi: 10.1364/ao.50.006319.
[34] V. V. Semak, A. Gerakis, M. N. Shneider, Measurement of temperature dependent absorption coefficient of water at 1064nm wavelength, *AIP Advances*, 2019, **9**, 085016, doi: 10.1063/1.5085746.
[35] W. Zhang, D. Qiao, F. Shi, C. Song, B. Wang, Y. Zhang, C. Luo, Research on small-size laser damage repairing process for fused silica optics, Fifth International Symposium on High Power Laser Science and Engineering (HPLSE 2023), October 16-19, 2023, Suzhou, China, SPIE, doi: 10.1117/12.3015273.
[36] S. Wang, W. Wang, Y. Xu, X. Zhang, C. Chen, P. Geng, N. Ma, Effect of nanosecond pulsed laser parameters on texturing formation of metallic surface: Experiment and modelling, *Journal of Materials Research and Technology*, 2023, **26**, 7775-7788, doi: 10.1016/j.jmrt.2023.09.118.
[37] W. M. Steen, Laser material processing, London: Springer London, 2003, doi: 10.1007/978-1-4471-3752-8.
[38] W. Charee, V. Tangwarodomnukun, Dynamic features of bubble induced by a nanosecond pulse laser in still and flowing water, *Optics & Laser Technology*, 2018, **100**, 230-243, doi: 10.1016/j.optlastec.2017.10.019.